Okhotsk Sea and Polar Oceans Research 8 (2024) 8-16

https://doi.org/10.57287/ospor.8.8

Article

Intra-seasonal and interannual variations of sea ice along the Okhotsk coast of Hokkaido from the viewpoint of atmospheric circulation

Yuki ASAZUMA[1], Masaya KURAMOCHI[1], and Hiroaki UEDA[2]

[1] *Graduate School of Science and Technology, University of Tsukuba, Tsukuba, Japan*
[2] *Faculty of Life and Environmental Sciences, University of Tsukuba, Tsukuba, Japan*

(Received September 29, 2023; Revised manuscript accepted January 16, 2024)

Abstract

In this study, we analyzed the intra-seasonal variations in sea ice along the Okhotsk coast of Hokkaido and clarified its relationship with atmospheric circulation fields based on observational data at Abashiri for 63 years (1958–2020). The results show that sub-weekly timescale variations are related to transient atmospheric disturbances that induce meridional winds and drive the sea ice near Hokkaido. When sea ice approaches the coast, atmospheric fields are marked by northerly winds to the rear of the developing extratropical cyclones that pass eastward near Japan. However, sea ice leaving the coast results from a southerly anomaly due to the weakened Siberian High and eastward-moving anticyclone. This study also investigated the interannual variations in sea ice along the coast of Hokkaido. During heavy sea-ice years, intensification of the Aleutian Low is discernable associated with northerly anomalies over the Okhotsk Sea and the enhancement of cold air intrusion toward Hokkaido. Simultaneously, diabatic cold air mass (CAM) genesis indicates that the accumulation of CAM near Hokkaido can be ascribed to an increase in the insulation effect due to the presence of sea ice. These findings provide the combined effect of the anomalous atmospheric fields and sea-ice insulation effect could be responsible for the significant negative correlation between air temperature and sea ice on the coast of Hokkaido.

Keywords: sea ice, Okhotsk Sea, Hokkaido, intra-seasonal variation, interannual variation

1. Introduction

The Okhotsk Sea (OS) is located in the western North Pacific and is characterized by seasonal sea ice. Climatologically, sea ice forms along the coast of Siberia because of the northwesterly winter winds. Sea ice drifts southward along the eastern coast of the Sakhalin Peninsula and reaches the coast of Hokkaido (COH) between January and March. Coastal sea ice near Hokkaido affects socio-economic activities, including sightseeing, around the Shiretoko World Heritage Site.

It is widely accepted that surface wind is one of the main factors that drives sea-ice motion, which is nearly parallel to the wind (Kimura and Wakatsuchi, 1999, 2000; Simizu *et al*., 2014). Thus, many previous studies on sea-ice variability in the OS have focused on atmospheric circulation. It has been indicated that the intensity of the Aleutian Low accompanied by anomalous northerly winds over the OS is closely associated with the interannual variation in the Okhotsk sea-ice extent (Tachibana *et al*., 1996; Yamazaki, 2000; Ueda *et al*., 2023). Yamazaki (2000) and Ogi and Tachibana (2006) suggested a relationship between interannual sea ice variability and the Arctic Oscillation (AO; Thompson and Wallace, 1998)/North Atlantic Oscillation. Ueda *et al*. (2023) indicated that a wave train forced by tropical convective heating affected the Okhotsk sea-ice variation. The anomalous sea-ice extent in the OS also affects the large-scale atmospheric circulation over the North Pacific through the supply/isolation of anomalous heat flux from the ocean surface to the atmosphere, which excites atmospheric Rossby waves (Honda *et al*., 1999). On a daily to weekly time scale, Kamae *et al*. (2023) pointed out that the rapid reductions in sea-ice extent in the OS are linked to surface easterly winds over the OS associated with eastward-moving extratropical cyclones.

These studies focused on the variation in sea-ice extent over the entire OS. Coastal sea ice with thinner ice and lower sea-ice concentration (SIC), such as sea ice near the COH (Toyota *et al*., 2022), is known to respond more strongly to atmospheric forcing as the response of sea ice to wind stress depends on ice thickness (Schevchenko *et al*., 2004). It has been reported that the SIC in the northern to middle OS and along the COH varies in an opposite manner on daily-to-weekly (Kamae *et al*., 2023) and year-to-year time scales (Aota *et al*., 1988; Honda, 2007). On an intra-seasonal timescale, Aota *et al*. (1988) showed that rapid increases and decreases in sea ice along the COH correspond to the surface pressure gradient between Wakkanai (the northernmost city of Hokkaido) and Nemuro (the easternmost city of Hokkaido) associated with inshore and offshore winds. Toyoda *et al*. (2022) indicated that variations in the first appearance/final disappearance

date are closely associated with variations in the Aleutian Low with meridional wind anomalies over the OS. It is also well known that sea ice along the COH is related not only to the meridional wind but also to the surface air temperature (SAT) near Hokkaido (Aota *et al*., 1988; Takahashi *et al*., 2011; Toyoda *et al*., 2022).

Although previous studies have suggested the importance of meridional winds in sea ice variation along the COH, the daily-to-weekly wind variation relevant to large-scale atmospheric circulation has not yet been clarified. Therefore, the main objective of this study is to clarify the atmospheric circulation pattern that produces intra-seasonal variations in sea ice along the COH. Climatologically, the western North Pacific is characterized by a storm track due to its high lower-tropospheric baroclinicity (*e.g*. Chen *et al*., 1991; Nakamura and Sampe, 2002). We hypothesize that the developing transient atmospheric disturbances induce the Wakkanai-Nemuro pressure gradient and meridional winds, as shown by Aota *et al*. (1988), which contribute to intra-seasonal variations in sea ice along the COH. Moreover, we discuss the interannual sea ice variability along the COH in comparison to its intra-seasonal variation.

2. Data

In this study, we used daily SIC data for 1958–2020 based on direct observations at Abashiri conducted by the Japan Meteorological Agency (JMA), which widely captures SIC variations along the COH on yearly and sub-weekly time scales (Aota *et al*., 1988; Toyoda *et al*., 2022). Moreover, the Abashiri Local Meteorological Observatory provides the SIC data for the longest period in comparison with that of the other meteorological observatories that face the OS such as Kitami-Esashi, Omu and Mombetsu. The data were obtained from visual observations at Abashiri at 9 a.m. within the range of 20 km from the Abashiri observatory and are indicated by 0–10, including locally formed ice up to 1. These data enabled us to analyze sea ice variations including the period before the start of satellite observations. Moreover, we used daily SIC data derived from the NOAA Optimum Interpolation Sea Surface Temperature V2 for 1981–2020 (Reynolds *et al*., 2002) to confirm the SIC duration in the OS. Based on these daily SICs, we calculated the yearly-accumulated SIC (YA-SIC), which is often used as an index of interannual variation in sea ice along the COH (Aota *et al*., 1988; Takahashi *et al*., 2011; Toyoda *et al*., 2022). The start and end dates of sea-ice existence at Abashiri for 1958–2020, provided by the JMA, were also used.

The atmospheric dataset used in this study was the Japanese 55-year Reanalysis (JRA-55; Kobayashi *et al*., 2015) from 1958 to 2020. This study utilized the definition of cold air mass (CAM) based on a specific isentropic surface θ_T (Iwasaki *et al*., 2014), which is a useful tool for diagnosing coldness and cold airflows. The amount of CAM is defined as

$$DP \equiv p_s - p(\theta_T), \tag{1}$$

where p_s is the surface pressure and $p(\theta_T)$ the pressure on the θ_T surface. The CAM conservation equation is as follows:

$$\frac{\partial}{\partial t} DP = -\boldsymbol{\nabla} \cdot \int_{p(\theta_T)}^{p_s} \mathbf{v}\, dp + G(\theta_T), \tag{2}$$

The CAM amount changes results from horizontal convergence of CAM flux (**MF**) and the diabatic heating rate ($G(\theta_T)$) which are defined as follows:

$$\mathbf{MF} = \int_{p(\theta_T)}^{p_s} \mathbf{v}\, dp, \tag{3}$$

and

$$G(\theta_T) = \frac{\partial p}{\partial \theta} \dot{\theta}\bigg|_{\theta_T}, \tag{4}$$

where $\mathbf{v} = (u, v)$ is the horizontal wind vector with the zonal wind u and the meridional wind v, and $\dot{\theta}$ indicates the diabatic heating rate. The diabatic change rate (Eq. 4) is the source of the CAM (hereafter referred to as the CAM genesis/loss). The threshold potential temperature θ_T is set to 280 K, following previous studies (*e.g*. Iwasaki *et al*., 2014; Ueda *et al*., 2023). SAT observational data at Abashiri, provided by the JMA, from 1958 to 2020 were used.

3. Climatology and intra-seasonal variations

3.1 Characteristics of sea ice along the COH

First, we examined the climatological sea-ice duration along the COH. Figure 1 shows the distribution of the climatological mean YA-SIC values. The YA-SIC east of Sakhalin exhibits larger values associated with sea ice drifting from the northern part of the OS to nearby Hokkaido due to the East Sakhalin Current (Simizu *et al*., 2014). The YA-SIC was larger in the eastern part of the

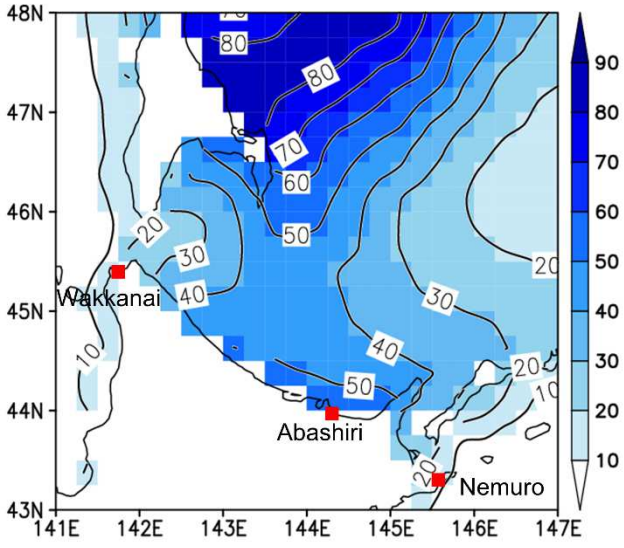

Fig. 1 Climatological mean YA-SIC from 1980/81 to 2019/20 (December–May) based on NOAA OISST V2.

Table 1. Monthly correlation coefficients of monthly SIC at Abashiri.

	start dates	DEC–JAN	FEB	MAR	APR–MAY	YA-SIC
start dates	1.000	−0.667	−0.490	−0.239	0.025	−0.488
DEC–JAN		1.000	0.574	0.216	0.033	0.623
FEB			1.000	0.563	0.272	0.840
MAR				1.000	0.693	0.856
APR–MAY					1.000	0.613
YA-SIC						1.000

COH than in the northern part. The locally long and high SIC is induced by the dam effect in the Shiretoko Peninsula (Aota *et al.*, 1988; Takahashi *et al.*, 2011).

We also analyzed the persistence of sea ice from winter to the following spring. Table 1 shows the monthly correlation coefficients of SIC at Abashiri. As for the month-wise correlation, positive correlations were salient, indicating the persistence of SIC in the COH for approximately two months. Moreover, the correlation between the start date and monthly SIC was negative from December to March, indicating that the earlier the first date, the larger the monthly SIC. These characteristics are consistent with the persistence of sea ice throughout the OS (Yamazaki, 2000; Ueda *et al.*, 2023).

3.2 Intra-seasonal variations of COH sea ice

Figure 2 shows the daily variation in SIC during 2019/20 winter as a sample. Sea ice along the COH exhibited large and rapid intra-seasonal variability. In this subsection, a composite analysis is performed on the day when sea ice rapidly approaches or leaves the COH during the sea ice season [hereafter referred to as approaching day (AD) and leaving day (LD), respectively]. Rapid variations are regarded as periods in which the SIC at Abashiri increases or decreases by five or more within three days. In this period, ADs and LDs were defined as the first days when the SIC

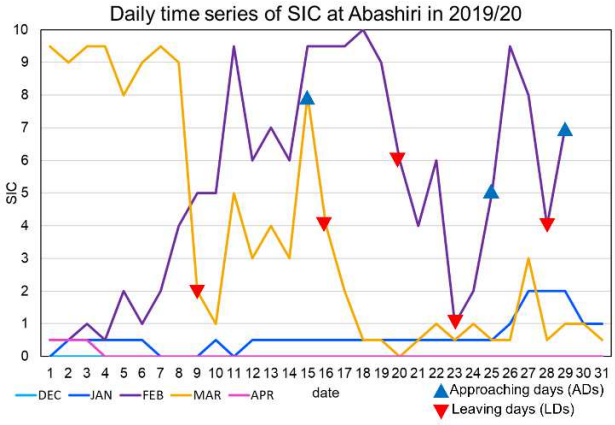

Fig. 2 Time series of daily SIC in 2019/20 from December to May. Triangles and inverted triangles denote approaching days (ADs) and leaving days (LDs), respectively.

increased and decreased by three or more, respectively. For the setting of the criteria, we have visually checked the daily variation of SIC and its spatial distribution for all years. We extracted 280 and 283 days for the ADs and LDs, respectively, during the 63-yr analysis period.

Figure 3 shows the temporal evolution of the anomalous atmospheric circulation [*i.e.* sea level pressure (SLP), surface horizontal wind, and geopotential height at 250 hPa (Z250)] around AD (day 0). Composite anomalies were defined as departures from the climatological mean for the corresponding calendar days. On day −2, an anomalous cyclone, located nearby Japan, moves eastward with developing and is accompanied with northerly winds nearby Hokkaido from day −1 to day 0. The horizontal SLP gradient around the cyclone was weak before the cyclone passed across Hokkaido but it strengthened after the center reached east of Hokkaido and subsequent intensification of the northerly wind, which induced a significant northerly wind in the rear part of the cyclone. The negative anomaly of Z250 was also salient to the west of the surface cyclone, and the upper-level trough gradually approached the surface cyclone while the cyclone moved eastward over the OS. This feature is indicative of a typical vertical structure in the developing stage relevant to baroclinic instability. The coupling of the surface cyclone and upper-level trough is often observed over the western North Pacific during winter and plays an important role in (explosively) developing cyclones, such as the Sea of Japan cyclone and the south coast cyclone (Nitta and Yamamoto, 1973; Takayabu, 1991). Using a numerical model, Kawano and Kawamura (2018) revealed that the anomalous sea-ice extent in the OS enhances the northerly winds to the rear of the cyclone. Considering their findings, it is implicated that the presence of a two-way interaction between transient cyclones and sea ice.

Figure 4 shows the temporal evolution of the anomalous atmospheric circulation around the LD. From day −2 to day 0, negative and positive SLP anomaly locates over the Eurasian continent toward the west of Japan and in the east of Japan, respectively, which produce a westward pressure gradient force and geostrophically balance the southerly wind anomaly nearby Hokkaido. The positive Z250 anomaly was also discernable west of the surface anticyclone. Moreover,

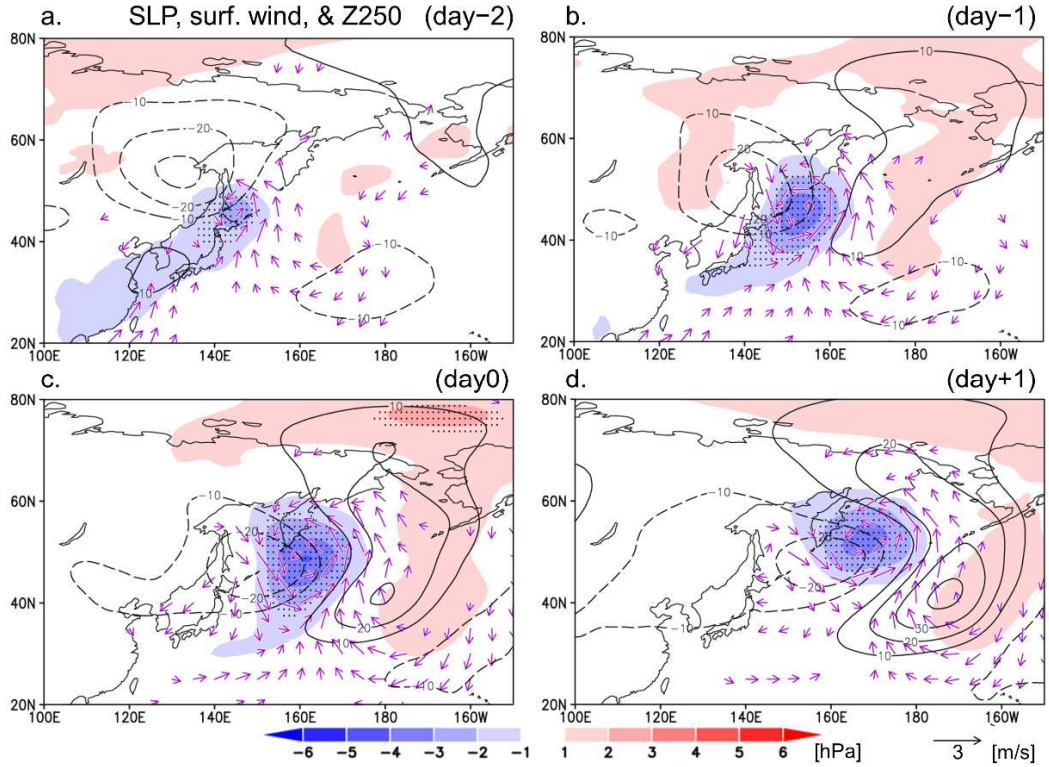

Fig. 3 Lagged composite anomalies for the days relative to the approaching days (ADs; day 0) in which shading denotes SLP (hPa), contours denote Z250 (interval: 10 m), and vectors denote the surface horizontal winds (m s^{-1}). The vectors less than 0.5 m s^{-1} were omitted. Stippling denotes the SLP anomalies significant at a 95% confidence level.

the upper-level ridge gradually approached the surface anticyclone, while the anticyclone moved eastward. Prior to the LD (day −2), the negative SLP anomaly indicates a weakening of the Siberian High together with the negative Z250 anomaly over northern Siberia. This feature is consistent with the anomalous vertical structure that contributes to the development and weakening of the Siberian High, as shown by Takaya and Nakamura (2005). In general, the attenuated Siberian High was responsible for the warmer climate over the Far East. Therefore, it is conceivable that the sea ice leaving the Okhotsk coast is also caused by in situ sea ice melting as well as southerly wind-induced ice drift.

4. Interannual variations of sea ice along the COH

The previous section demonstrated the importance of transient atmospheric disturbances on sub-weekly scale sea ice variations in the COH. However, the correlation between the AD/LD frequency during the sea ice season and the interannual variability of the YA-SIC was weak ($r = 0.18/0.17$). This suggests that intra-seasonal and interannual variations are controlled by different mechanisms.

A composite analysis was performed based on the YA-SIC index at Abashiri, which represents the year-to-year variability of sea ice along the COH. Figure 5 shows the year-to-year variations in YA-SIC at Abashiri from 1958 to 2020. The 1958 YA-SIC included SIC in December 1957. The heavy sea-ice years are defined as YA-SIC exceeding 1 standard deviation and light sea ice years are defined as that below −1 standard deviation compared with the climatology. The standard deviation of the YA-SIC was 179.36 for 1958–2020. The standard deviation is widely adopted as the threshold to analyze interannual climate variations (*e.g.* Ueda *et al.,* 2023). On the basis of these criteria, 12 years (1961, 1963, 1964, 1965, 1970, 1977, 1978, 1979, 1981, 1984, 1986, 2003) are defined as the heavy sea-ice years. Likewise, 11 years (1989, 1990, 1991, 1992, 2004, 2006, 2007, 2009, 2010, 2016, 2020) are picked as the light sea-ice years. Notably, all heavy sea-ice years occurred before 2003, whereas seven of the 11 light sea-ice years occurred after 2003. Moreover, the YA-SIC at Abashiri clearly showed significant long-term decreasing trends (−65.12/decade), implicating the influence of anthropogenic global warming. Composite maps were then constructed based on the January–March atmospheric circulation fields as the climatological start and end dates of the sea-ice existence at Abashiri for 1958–2020 were January 18 and April 9, respectively. The composite anomaly fields represent the deviations from the 63-yr climatology for January to March.

Figure 6 depicts the spatial distribution of YA-SIC anomalies. Note that the anomalies were computed for the heavy and light sea-ice years after 1980, owing to the data variable period. The SIC in the southern part of the

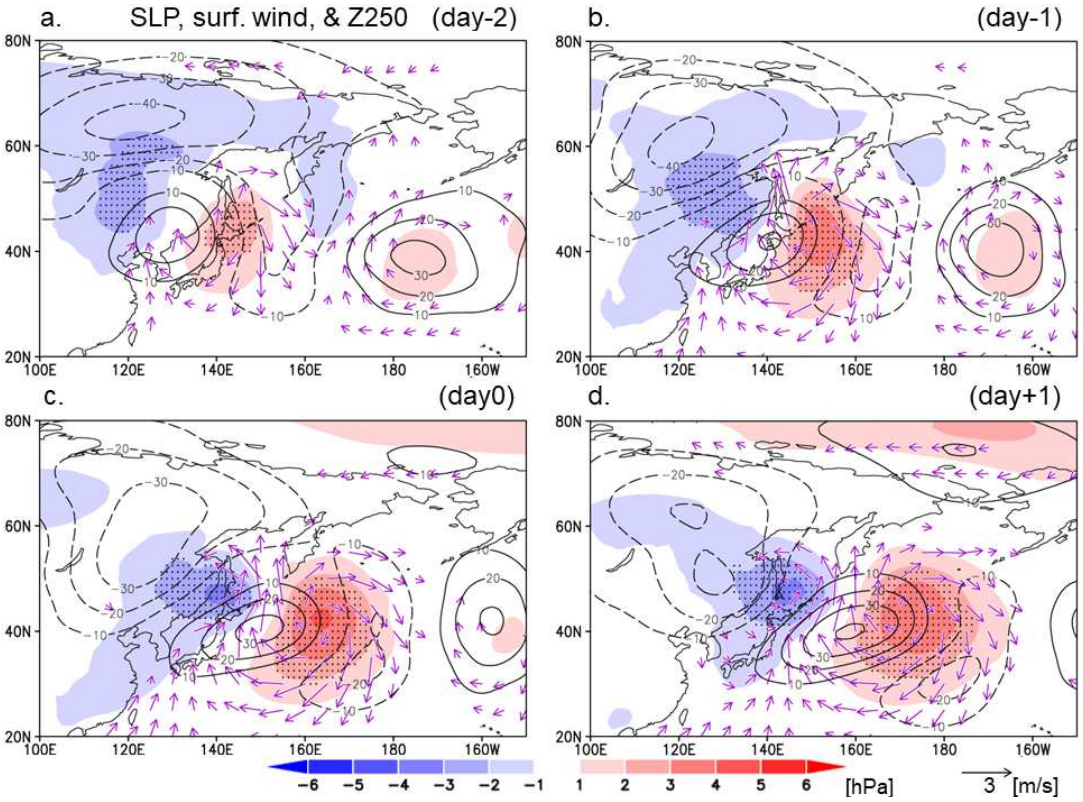

Fig. 4 Same as Fig. 3, but for the leaving days (LDs).

OS shows similar variations to the SIC along the COH. Interestingly, the YA-SIC in the heavy sea-ice year (Fig. 6a) shows a positive anomaly over the southern OS and a negative anomaly in the northern OS, which is consistent with the results of previous studies addressing sea ice before 1989 (Aota *et al*., 1988; Honda, 2007). However, the YA-SIC in the light sea-ice year (Fig. 6b) showed a negative anomaly over the entire OS.

Figure 7 shows the composite anomalies of atmospheric circulations near the ground during years with heavy and light sea ice. For the heavy sea-ice years (Fig. 7a), the intensification of the Aleutian Low, together with the anomalous northerly over the OS, is significant. This situation may be favorable for sea ice approaching the COH. The converse was true for light sea-ice years (Fig. 7b). Moreover, we did not find a significant anomaly in the Siberian High, which differs from the LD results. These results indicate that the intensity of the stationary Aleutian Low influences the interannual variability of sea ice along the COH as well as that of the entire OS (Yamazaki, 2000; Ueda *et al*., 2023). However, if we take a close look at the anomalous

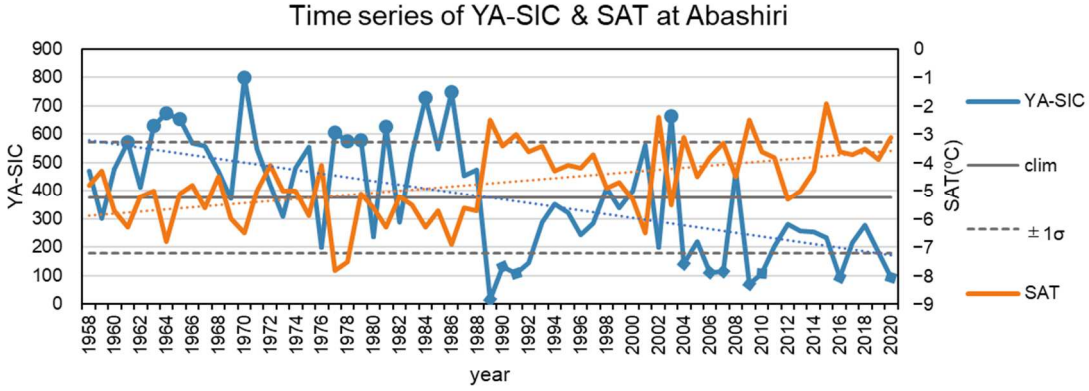

Fig. 5 Time series of Interannual variations of YA-SIC (blue) and SAT (orange) at Abashiri in from 1958 to 2020. Dotted lines indicate their linear trends by the corresponding color. Horizontal solid and dashed lines denote the climatological mean and 1 standard deviation of YA-SIC. SAT was averaged from January–March. Filled circles and diamonds denote the extracted heavy and light sea-ice years, respectively, in this study.

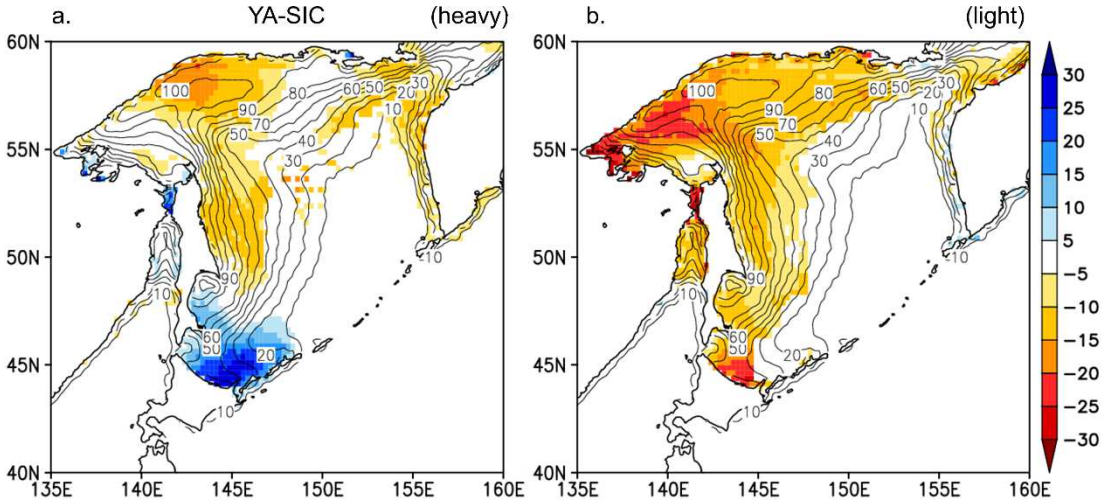

Fig. 6 Composite anomalies of YA-SIC (shading) in (a) heavy and (b) light sea ice years based on NOAA OISST V2. Contours indicate climatological YA-SIC in 1982–2020.

circulation fields in comparison with those in Ueda *et al.* (2023), there were local differences between the sea-ice variation in the COH and the entire OS. As for the wind direction, the anomalies relevant to the sea ice along the COH exhibited northeasterly (southwesterly) in the heavy (light) years (Fig. 7), whereas those in the entire OS were westerly (easterly) in its heavy (light) years (Ueda *et al.*, 2023). These differences are consistent with the locality of the SLP anomalies. The northeast-southwest direction of the wind variation is more effective for the sea ice approaching/leaving the COH and subsequent interannual variability.

It is widely accepted that sea ice along the COH is closely related to the local air temperature (Fig. 5; Aota *et al.*, 1988; Takahashi *et al.*, 2011). The correlation coefficient of YA-SIC at Abashiri against the mean air temperature at Abashiri in January–March was –0.81. We diagnosed the formation processes of the relationship between SAT and sea ice using the CAM. The local CAM and SAT are highly correlated (Abdillah *et al.* 2018), and the CAM has an advantage in assessing the diabatic change in coldness (Eq. 2). Figures 8a and 8b show the composite anomalies of the CAM amounts and flux. In heavy sea-ice years (Fig. 8a), the CAM amount was significantly larger than normal near Hokkaido. The southwestward CAM flux anomaly from Alaska to the OS is consistent with the anomalous winds based on the effects of the intensification of the Aleutian Low, which indicates that the intensification of the Aleutian Low promotes the enhancement of cold air intrusion toward Hokkaido. In addition, the positive CAM genesis anomaly near COH was significant (Fig. 8c). This anomaly indicates the crucial role of an increase in the heat insulation effect (Martin *et al.*, 1998; Nihashi *et al.*, 2009) along the COH in the accumulation of CAM. In other words, the sea-ice insulation effects during heavy sea-ice years created an obstacle for heat gain to the atmosphere from the relatively warmer ocean, which

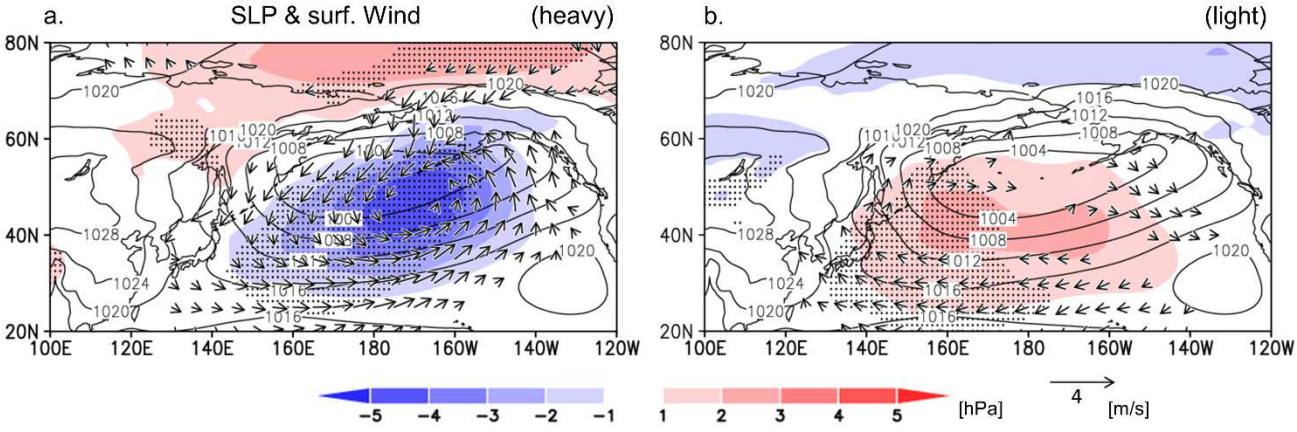

Fig. 7 (a) Composite anomalies in the heavy sea ice years of SLP (shading; hPa) and surface horizontal winds (vectors; m s^{-1}). The vectors less than 0.5 m s^{-1} were omitted. Stippling denotes the SLP anomalies significant at a 95% confidence level. Contours denote January–March mean of the climatological SLP (interval: 4 hPa). (b) Same as (a), but for the light sea-ice years.

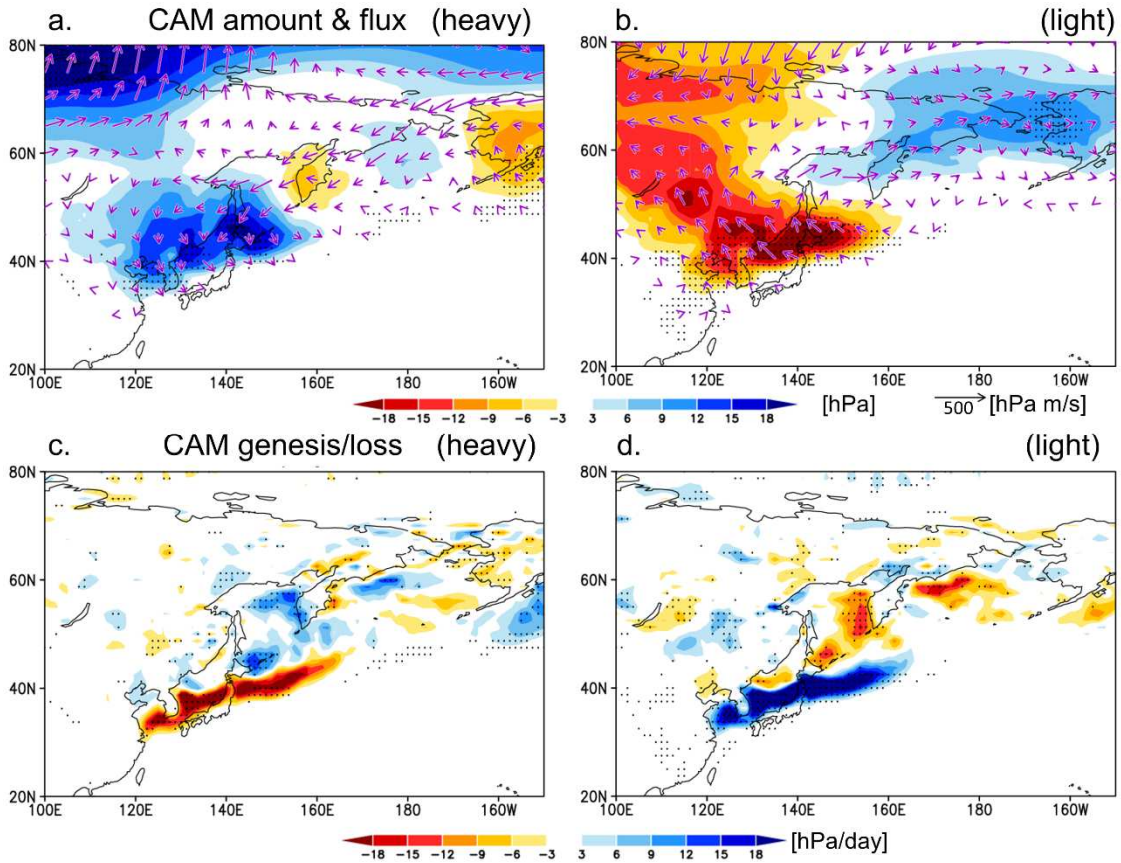

Fig. 8 (a) Composite anomalies in the heavy sea-ice years of CAM amount (shading; hPa) and CAM flux (vectors; hPa m s^{-1}) below 280 K. Stippling denotes the CAM amount anomalies significant at a 95% confidence level. (b) Same as (a), but for the light sea-ice years. (c) Composite anomalies in the heavy sea-ice years of the CAM genesis/loss (shading; hPa day^{-1}) below 280 K. Stippling denotes the CAM genesis/loss anomalies significant at a 95% confidence level. (d) Same as (c), but for the light sea-ice years.

would have contributed to the prominent cold anomalies in the southern OS. As for the light sea ice years (Fig. 8b), the amount of CAM was significantly lower near Hokkaido and over the Sea of Japan, implicating that the sea ice along the COH tends to melt easily. The CAM flux exhibits an anomalous anticyclonic circulation over the OS, including the anomalous southeasterly across the COH toward the Sea of Japan. The continental northwestward anomalies of CAM flux indicate a decrease in cold air outbreaks from East Asia. The negative anomalies of CAM genesis over the eastern and southern OS were due to the decrease in sea ice for the light years (Fig. 8d).

5. Summary and conclusions

We investigated seasonal variations in sea ice along the COH based on the Abashiri SIC over the last 63 years (1958–2020). According to the findings of this study, the intra-seasonal variation in sea ice along the COH is accompanied by meridional wind anomalies due to transient atmospheric disturbances. Sea ice approaching the coast results from northerly winds to the rear of a developing extratropical cyclone that passes eastward near Japan. The cyclones detected in the present study can be ascribed to local depressions, such as the Sea of Japan cyclone or the south coast cyclone. In contrast, sea ice leaving the coast was dominated by a southerly anomaly owing to the weakened Siberian High and eastward-moving anticyclone. The weakening of the Siberian High was accompanied by a negative Z250 anomaly over northern Siberia, which resulted in mild weather conditions over the Far East. This study revealed the importance of atmospheric baroclinic waves on sub-weekly timescale sea-ice variations in the COH.

We also analyzed the interannual variability in sea ice along the COH. Heavy sea-ice years are characterized by the deepening of the Aleutian Low, which is accompanied by northeasterly winds and southward CAM flux anomalies toward Hokkaido. The composite anomaly of CAM genesis shows a significant positive anomaly near the COH, which implicates that the accumulation of CAM near Hokkaido is ascribed to an increase of the insulation effect due to the presence of sea ice. In contrast, the light sea-ice years displayed a weakening of the Aleutian Low and a decrease in diabatic CAM genesis. Thus, it is suggested that the

insulation effect caused by the presence of sea ice is responsible for the negative correlation between SAT and sea ice in Hokkaido. Simultaneously, the fluctuation in the Aleutian Low brings cold air and sea ice toward the COH. A deeper understanding of the atmospheric fields associated with sea-ice movement will improve prediction on a corresponding timescale and help interpret the responses of sea ice in the COH to climate change.

The YA-SIC at Abashiri clearly shows significant long-term decreasing trends together with increasing SAT trends (Fig. 5), in association with global warming. Recently, Tamura and Sato (2023) showed that the significantly increasing SAT trend over Japan, especially for days when cold air advection from the OS dominates, is associated with the retreat of OS sea ice. Our results on the interannual relationship between SAT and sea ice along the COH are consistent with their findings regarding the global warming trend. Therefore, it is essential to specify the process of decreasing sea-ice trends along the COH. As several time-scale variations in sea ice and the atmosphere include their interactions, further studies based on sensitivity experiments using numerical models are required to clarify causal relationship.

Acknowledgments

SIC observation data were provided by the JMA. The authors acknowledge Drs. Humio Mitsudera (Hokkaido University), Takahiro Toyoda (Meteorological Research Institute) and Takenobu Toyota (Hokkaido University) for providing helpful information on the sea ice along the COH. We thank Dr. Tatsuro Karaki (University of Tsukuba) for fruitful discussions on sea-ice variation from the viewpoint of the ocean. We also thank Ms. Hitomi Yoshida (Okhotsk Garinko & Tower Co., Ltd.) for providing helpful local information. This study was supported by the Environment Research and Technology Development Fund (JPMEERF20214002) of the Environmental Restoration and Conservation Agency of Japan and the Japan Society for the Promotion of Science KAKENHI (21H00626 / 21H01154). The second author (MK) is supported by the JSPS Research Fellowship for Young Scientists.

References

Abdillah, M. R., Y. Kanno, and T. Iwasaki (2018): Strong linkage of El Niño–Southern Oscillation to the polar cold airmass in the Northern Hemisphere. *Geophys. Res. Lett.*, **45**, 5643–5652.

Aota, M., M. Ishikawa, and E. Uematsu (1988): Variation in ice concentration off Hokkaido Island. *Low Temp. Sci., Ser. A*, **47**, 161–175.

Chen, S. J., Y.-H. Kuo, P.-Z. Zhang, and Q.-F. Bai (1991): Synoptic climatology of cyclogenesis over East Asia, 1958–1987. *Mon. Wea. Rev.*, **119**, 1407–1418.

Honda, M. (2007): Relationship between the Okhotsk sea ice and atmospheric field. *Kishou Kenkyu Note*, **214**, 63–73 (in Japanese).

Honda, M., K. Yamazaki, H. Nakamura, and K. Takeuchi (1999): Dynamic and thermodynamic characteristics of atmospheric response to anomalous sea-ice extent in the Sea of Okhotsk. *J. Climate*, **12**, 3347–3358.

Iwasaki, T., T. Shoji, Y. Kanno, M. Sawada, M. Ujiie, and K. Takaya (2014): Isentropic analysis of polar cold airmass streams in the northern hemispheric winter. *J. Atmos. Sci.*, **71**, 2230–2243.

Kamae, Y., H. Ueda, T. Inoue, and H. Mitsudera (2023): Atmospheric circulations associated with sea-ice reduction events in the Okhotsk Sea. *J. Meteor. Soc. Japan*, **101**, 125–137.

Kawano, T., and R. Kawamura (2018): Influence of Okhotsk sea ice distribution on a snowstorm associated with an explosive cyclone in Hokkaido, Japan. *SOLA*, **14**, 1–5.

Kimura, N., and M. Wakatsuchi (1999): Processes controlling the advance and retreat of sea ice in the Sea of Okhotsk. *J. Geophys. Res.*, **104**, 11137–11150.

Kobayashi, S., and 11 co-authors (2015): The JRA-55 reanalysis: General specifications and basic characteristics. *J. Meteor. Soc. Japan*, **93**, 5–48.

Martin, S., R. Drucker, and K. Yamashita (1998): The production of ice and dense shelf water in the Okhotsk Sea polynyas. *J. Geophys. Res.*, **103**, 27771–27782.

Nakamura, H., and T. Sampe (2002): Trapping of synoptic-scale disturbances into the North-Pacific subtropical jet core in midwinter. *Geophys. Res. Lett.*, **29**, doi: 10.1029/2002GL015535.

Nitta, T., and J. Yamamoto (1974): On the observational characteristics of intermediate scale disturbances generated near Japan and the vicinity. *J. Meteor. Soc. Japan*, **52**, 11–31.

Nihashi, S., K. I. Ohshima, T. Tamura, Y. Fukamachi, and S. Saitoh (2009): Thickness and production of sea ice in the Okhotsk Sea coastal polynyas from AMSR-E. *J. Geophys. Res.*, **114**, C10025.

Ogi, M., and Y. Tachibana (2006): Influence of the annual Arctic Oscillation on the negative correlation between Okhotsk Sea ice and Amur River dis-charge. *Geophys. Res. Lett.*, **33**, L08709.

Reynolds, R. W., N. A. Rayner, T. M. Smith, D. C. Stokes, and W. Wang (2002): An improved in situ and satellite SST analysis for climate. *J. Climate*, **15**, 1609–1625.

Schevchenko, G. V., A. B. Rabinovich, and R. E. Thomson (2004): Sea-ice drift on the northeastern shelf of Sakhalin Island. *J. Phys. Oceanogr.*, **34**, 2470–2491.

Simizu, D., K. I. Ohshima, J. Ono, Y. Fukamachi, and G. Mizuta (2014): What drives the southward drift of sea ice in the Sea of Okhotsk? *Prog. Oceanogr.*, **126**, 33–43.

Tachibana, Y., M. Honda, and K. Takeuchi (1996): The abrupt decrease of the sea ice over the southern part of the Sea of Okhotsk in 1989 and its relation to the recent weakening of the Aleutian low. *J. Meteor. Soc. Japan*, **74**, 579–584.

Takahashi, S., T. Kosugi, and H. Enomoto (2011): Sea-ice extent variation along the coast of Hokkaido, Japan: Earth's lowest-latitude occurrence of sea ice and its relation to changing climate. *Ann. Glaciol.*, **52**, 165–168.

Takaya, K., and H. Nakamura (2005): Mechanisms of intraseasonal amplification of the cold Siberian high. *J. Atmos. Sci.*, **62**, 4423–4440.

Takayabu, I. (1991): "Coupling development": An efficient mechanism for the development of extratropical cyclones. *J. Meteor. Soc. Japan*, **69**, 609–628.

Tamura, K., and T. Sato (2023): Localized strong warming and humidification over winter Japan tied to sea ice retreat. *Geophys. Res. Lett.*, **50**, e2023GL103522.

Thompson, D. W. J., and J. M. Wallace (1998): The Arctic

Oscillation signature in the wintertime geopotential height and temperature fields. *Geophys. Res. Lett*., **25**, 1297–1300.
Toyoda, T., Y. Kitamura, and R. Okada (2022): Sea ice variability along the Okhotsk coast of Hokkaido based on long-term JMA meteorological observatory data. *Okhotsk Sea and Polar Oceans Research*, **6**, 27–35.
Toyota, T., N. Kimura, J. Nishioka, M. Ito, D. Nomura, and H. Mitsudera (2022): The interannual variability of sea ice area, thickness, and volume in the southern Sea of Okhotsk and its likely factors. *J. Geophys. Res.: Oceans*, **127**, e2022JC019069.
Ueda, H., M. Kuramochi, and H. Mitsudera (2023): Interannual variations of sea-ice extent in the Okhotsk Sea—A pan-Okhotsk climate system perspective. *Atmosphere-Ocean*, **61**, 234-245.
Yamazaki, K. (2000): Interaction between the wintertime atmospheric circulation and the variation in the sea ice extent of the Sea of Okhotsk. *Seppyo*, **62**, 345–354 (in Japanese).

Summary in Japanese

和文要約

オホーツク沿岸海氷の季節内・年々変動と大気循環場

朝妻勇貴[1]，倉持将也[1]，植田宏昭[2]

[1]筑波大学理工情報生命学術院，[2]筑波大学生命環境系

北海道オホーツク沿岸海氷の季節内変動および年々変動と大気循環場の関係を調査した。事例合成解析の結果、北海道沿岸海氷の季節内変動は、日本付近を東進する移動性擾乱がもたらす南北風偏差が影響していることが示された。海氷の接岸時には、日本付近を発達しながら東進する低気圧の後面で北風偏差が見られ、海氷の移動と整合的である。一方、離岸時は、シベリア高気圧の弱化と移動性高気圧の通過に伴う南風偏差が顕著であった。沿岸海氷の年々変動ついても調査した結果、多氷年ではアリューシャン低気圧の強化が確認された。同時にオホーツク海上で強化された北風に伴い、北海道への寒気流の強化が見られた。寒気質量の生成率偏差は、北海道沿岸で有意な正偏差を示し、海氷増加による海氷の断熱効果が北海道付近の寒気を増加させるように働く。北海道沿岸の海氷と気温の負の相関は、海氷の断熱効果と大気循環場の偏差の両者によりもたらされる事が示唆される。

Correspondence to: Y. ASAZUMA
s2321113@u.tsukuba.ac.jp.